Abstract—Fishing locations for Pacific saury (*Cololabis saira*) obtained from images of the Operational Linescan System (OLS) of the U.S. Defense Meteorological Satellite Program, together with maximum entropy models and satellite-based oceanographic data of chlorophyll-*a* concentration (chl-*a*), sea-surface temperature (SST), eddy kinetic energy (EKE), and sea-surface height anomaly (SSHA), were used to evaluate the effects of oceanographic conditions on the formation of potential fishing zones (PFZ) for Pacific saury and to explore the spatial variability of these features in the western North Pacific. Actual fishing regions were identified as the bright areas created by a 2-level slicing method for OLS images collected August–December during 2005–2013. The results from a Maxent model revealed its potential for predicting the spatial distribution of Pacific saury and highlight the use of multispectral satellite images for describing PFZs. In all monthly models, the spatial PFZ patterns were explained predominantly by SST (14–16°C) and indicated that SST is the most influential factor in the geographic distribution of Pacific saury. Also related to PFZ formation were EKE and SSHA, possibly through their effects on the feeding grounds conditions. Concentration of chl-*a* had the least effect among other environmental factors in defining PFZs, especially during the end of the fishing season.

Predicting potential fishing zones for Pacific saury (*Cololabis saira*) with maximum entropy models and remotely sensed data

Achmad F. Syah (contact author)[1,2]
Sei-Ichi Saitoh[1,3]
Irene D. Alabia[3]
Toru Hirawake[1]

Email address for contact author: fachrudinsyah@gmail.com

[1] Laboratory of Marine Environment and Resource Sensing
   Faculty of Fisheries Sciences
   Hokkaido University
   3-1-1 Minato-cho
   Hakodate 041-8611, Japan

[2] Department of Marine Science
   University of Trunojoyo Madura
   Jalan Raya Telang
   P.O. Box 2 Kamal
   Bangkalan-Madura, Indonesia

[3] Arctic Research Center
   Hokkaido University
   N21-W11 Kita-ku
   Sapporo 001-002, Japan

The Pacific saury (*Cololabis saira*) is widely distributed in the western North Pacific from subarctic to subtropical waters and is one of the commercially important pelagic species in Japan, Russia, Korea, and Taiwan. The total landings of this species in these countries increased from 171,692 metric tons (t) in 1998 to 449,738 t in 2011. Over the last half century, annual catches of Pacific saury in Japan, for example, have averaged around 257,800 t (Tian et al., 2003) and have fluctuated greatly from 52,207 t in 1969 to 207,770 t in 2011 (Fisheries Agency and Fisheries Research Agency of Japan, 2012).

The number, size, and location of fishing grounds for Pacific saury are largely affected by oceanographic conditions (Yasuda and Watanabe, 1994; Kosaka, 2000; Tian et al., 2002), and the significant effect of

environmental factors on abundance of Pacific saury was evident in the unexpected drop in both the catch and catch per unit of effort in 1998, following a period of high abundance (Tian et al., 2003). The distribution and migratory patterns of Pacific saury have been associated with chlorophyll-*a* (chl-*a*) concentration and sea-surface temperature (SST) (Watanabe et al., 2006; Mukai et al., 2007; Tseng et al., 2013). Moreover, sea-surface height indicates water mass movements and, by extension, the flow of heat and nutrients, which will subsequently influence productivity (Ayers and Lozier, 2010). Sea-surface height can also be used to infer physical oceanographic features, such as eddies, fronts, and convergences (Polovina and Howell, 2005). Therefore, understanding the relationship between oceanographic

factors and the migration and distribution of species is essential for fisheries management.

Most studies of Pacific saury have concentrated on distribution and migration and have used in situ or logbook data (Huang et al., 2007; Tseng et al., 2013), and models have been developed to investigate growth and abundance (Tian et al., 2004; Ito et al., 2004, 2007; Mukaietal., 2007). In contrast, Watanabe et al. (2006) proposed a spatial and temporal migration model for stock size that was dependent on SST. However, integrated high-resolution nighttime satellite images, such as those available in the time-series data from the Operational Linescan System (OLS) of the Defense Meteorological Satellite Program, U.S. Department of Defense, together with habitat and environmental modeling, have not been used to predict the potential fishing zones for Pacific saury.

In Japan, fishing vessels operate at night and use stick-held dip nets, locally known as *bouke ami*, which are equipped with lights to attract fishes (Fukushima, 1979). These fishing vessels, equipped with lights, as are vessels that fish for Pacific saury, can be identified by the OLS sensor, which also enables the detection of moonlight-illuminated clouds and lights from cities, towns, industrial sites, gas flares, and ephemeral events, such as fires and lightning-illuminated clouds (Elvidge et al., 1997). In addition, OLS nighttime images can be used to estimate fishing vessel numbers and fishing areas for squid (Kiyofuji and Saitoh, 2004; Kiyofuji et al., 2004). The relationship between the number of lit pixels in OLS nighttime images and the number of fishing vessels also has been analyzed for the fishery of *Illex argentinus* (Waluda et al., 2002). The brightly lit areas seen in nighttime images of the western North Pacific are the result of vessels fishing for Pacific saury or squid (Semedi et al., 2002; Saitoh et al., 2010; Mugo et al., 2014).

Predictive habitat modeling has become an increasingly useful tool for marine ecologists and conservation scientists in order to estimate the patterns of species distribution and to subsequently develop conservation strategies (Johnson and Gillingham, 2005; Tsoar et al., 2007; Ready et al., 2010). The maximum entropy method (Phillips et al., 2006) involves one of the most widely used machine-learning algorithms for inferring species distributions. In recent studies, the method of maximum entropy has been applied to both terrestrial (Peterson et al., 2007) and marine ecosystems (Ready et al., 2010; Edrén et al., 2010; Alabia et al., 2015). In this study, we used a maximum entropy approach with multi sensor satellite datasets and OLS-derived species occurrences to create an accurate prediction model and investigate the potential fishing zones for Pacific saury in the western North Pacific. The objectives of this study were to evaluate the effects of oceanographic factors on the formation of potential fishing zones for Pacific saury and to examine the variability in spatial patterns of potential fishing zones in relation to the prevailing oceanographic conditions in the western North Pacific.

Materials and methods

Study area

This study was conducted in the western North Pacific, extending from 140° to 155°E and from 34° to 46°N (Fig. 1). In this study area, located between the subarctic and subtropical domains of the North Pacific, the confluence of the warm Kuroshio Current and the cold Oyashio Current forms the Kuroshio–Oyashio transition zone (Roden, 1991), also called the subarctic–subtropical transition zone. The Kuroshio Current is characterized by warm, low-density, nutrient-poor, and high-salinity surface waters (Yatsu et al., 2013), whereas the Oyashio Current is characterized by low-salinity, low-temperature, and nutrient-rich waters (Sakurai, 2007). The Kuroshio–Oyashio transition zone is characterized by the mixing of various water masses and complex physical oceanographic structures (Roden, 1991). Moreover, 3 major oceanic fronts exist in this region: the Polar Front, Subarctic Front, and Kuroshio Extension Front (Science Council of Japan[1]). The characteristic patterns of these oceanic fronts also have been well documented in earlier studies (Kitano, 1972; Roden et al., 1982; Belkin and Mikhailichenko, 1986; Miyake, 1989; Belkin et al., 1992, 2002; Yoshida, 1993; Onishi, 2001; Murase et al., 2014; Shotwell et al., 2014).

Satellite nighttime images

Daily cloud-free OLS nighttime images were downloaded from the Satellite Image Database System of the Agriculture, Forestry and Fisheries Research Information Center of the Japan Ministry of Agriculture, Forestry and Fisheries [the system is no longer operating]. The images were then used to determine the location of the vessels that fish for Pacific saury in the western North Pacific. A TeraScan[2] system, vers. 4.0 (Seaspace Corp., Poway, CA) was used to analyze the images and to process the nighttime lights into digital numbers (DNs), in a range of 0–63, that represent the visible pixels in relative values. We selected 1264 single pass images collected from August through December during 2005–2013 (9 years) by 6 Defense Meteorological Satellite Program satellites (F13, F14, F15, F16, F17, and F18) (Table 1). The period from August through December was chosen for analysis because it corresponds with the fishing season of Pacific saury. To construct the habitat suitability model, the daily images were reprocessed with a 1-km resolution and then compiled in a monthly database. The location of the vessels was assumed to represent the location of Pacific saury.

Figure 1

Map of the study area in the western North Pacific with the hydrographic and topographic features of the ocean basin. The line with dashes and dots represents the boundary of the EEZ of Japan. The lines with dashes correspond to the 3 major oceanic fronts—the Polar Front (PF), Subartic Front (SAF), and Kuroshio Extension Front (KEF). The subarctic–subtropical transition zone is also shown. Redrawn after Murase et al. (2014).

Detection of fishing vessel

We examined the histograms of DNs in our analyses of OLS images for each month in order to identify the fishing areas. Several peaks in DNs were recorded over the examined 5-month periods (Fig. 2). To extract the areas with fishing-vessel lights, DN thresholds for identifying Pacific saury fishing vessels were calculated for each month because of the monthly differences in DN frequency distribution. A 2-level slicing method was used to extract the bright areas thought to be caused by the fishing fleet. This method is used to find a statistical optimum threshold from the DN frequency distribution (Takagi and Shimoda, 1991).

The thresholds, k, were determined through the use of the following method proposed by Kiyofuji and Saitoh (2004), and the variance, $\sigma^2(k)$, was calculated with the equations proposed by Takagi and Shimoda (1991):

$$\sigma^2(k) = \omega_0(\mu_0 - \mu_T)^2 + \omega_1 (\mu_1 - \mu_T)^2, \qquad (1)$$

where n_i = the number of pixels at i levels;
N = the total number of pixels;
P_i = n_i/N;
ω_0 = $\sum_{i=1}^{k} Pi$ and $\omega_1 = \sum_{i=k+1}^{l} Pi$;
μ_0 = $\sum_{i=1}^{k} iPi / \omega_0$ and $\mu_1 = \sum_{i=k+1}^{l} iPi / \omega_1$;
μ_T = $\sum_{i=1}^{l} iPi$.

With these methods, 5 thresholds were identified (Table 2). Class 1, 2, 3, and 4 thresholds indicate ocean water or cloud coverage, and the class 5 threshold indicates bright areas resulting from fishing vessel lights. Therefore, class 5 threshold values were applied to extract the bright areas that represented fishing vessel lights.

Lights from vessels that fish for Pacific saury and those that fish for squid are contained in OLS images. These lights are difficult to distinguish from each other; therefore, it is necessary to generate OLS images with less contamination from the lights of vessels fishing for

Table 1

Number of images from the Operational Linescan System of the U.S. Defense Meteorological Satellite Program for the period 2005–2013, by month and year, that were used in this study to predict fishing locations of Pacific saury (*Cololabis saira*) in the western North Pacific.

Month	2005	2006	2007	2008	2009	2010	2011	2012	2013
August	37	24	14	0	0	15	15	12	4
September	44	43	9	2	7	27	17	29	17
October	67	70	55	3	11	47	36	33	31
November	72	53	69	16	16	43	34	27	36
December	51	31	21	1	10	30	43	22	20

squid. In this study, we used SST to distinguish between the lights of the vessels that fish for Pacific saury and those of other fishing vessels because Pacific saury prefers colder areas for their migration routes (Saitoh et al., 1986) and this approach was used earlier by Mugo et al. (2014).

Because Pacific saury are distributed below the upper SST limit (Table 3), we split the nighttime light images into 2 categories. All lights that occurred above the upper SST limit were categorized as lights related to squid fishing, and all lights that occurred below this limit were assumed to be from vessels fishing for Pacific saury. Consequently, only the locations of lights that indicated fishing for Pacific saury were used for our habitat modeling procedures.

Environmental data

We used satellite-derived data—chl-*a*, SST, eddy kinetic energy (EKE), and sea-surface height anomaly (SSHA)—from 2005 through 2013 as environmental factors in the maximum entropy models. Daily chl-*a* and SST values were derived from satellite images from the Moderate Resolution Imaging Spectroradiometer (MODIS)-Aqua mission and were downloaded from NASA Goddard Space Flight Center [website]. These data were processed with the SeaDAS package, vers. 6.4 (NASA Goddard Space Flight Center, Greenbelt, MD) and reprocessed to create maps with a 1-km resolution.

Daily SSHA and geostrophic velocities (*u*, *v*) from the Topex/Poseidon and ERS-1/2 altimeters were
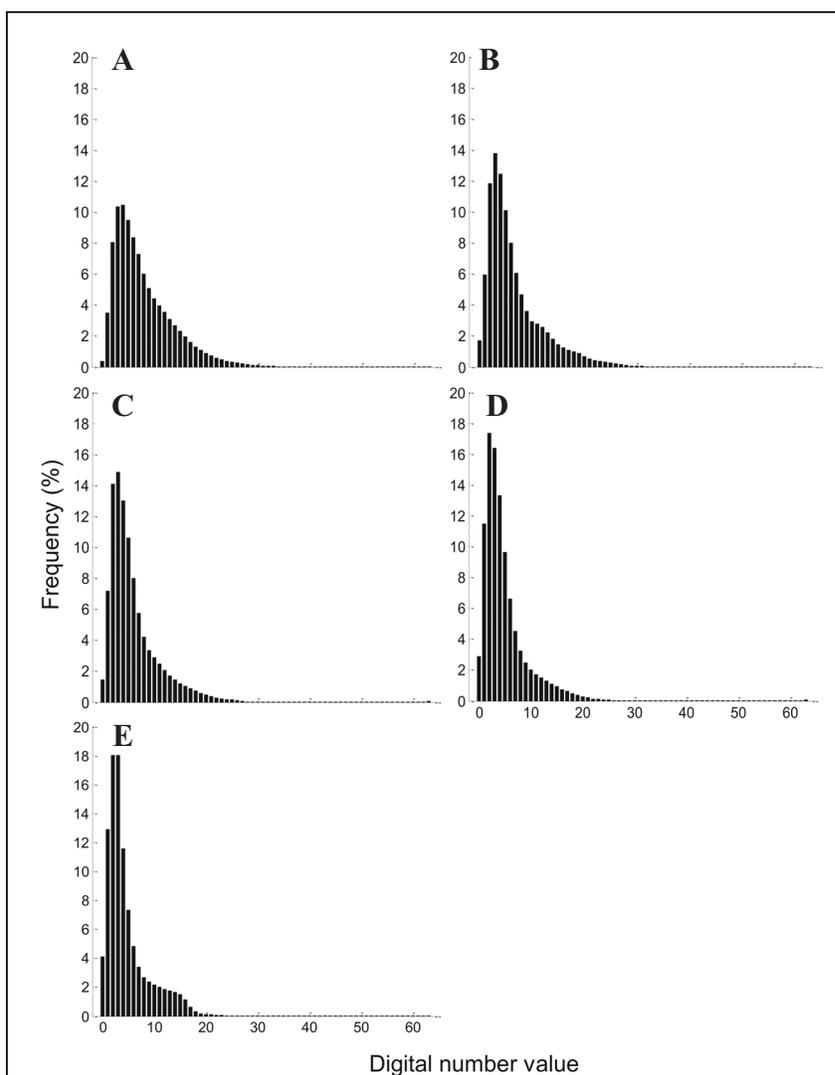
Figure 2

Histograms of the relative frequency of visible pixels derived from monthly composite images obtained from the western North Pacific from the Operational Linescan System of the U.S. Defense Meteorological Satellite Program for (**A**) August, (**B**) September, (**C**) October, (**D**) November, and (**E**) December for the period 2005–2013

Table 2

Thresholds for digital numbers (in pixels) for satellite images from the Operational Linescan System of the U.S. Defense Meteorological Satellite Program for the period 2005–2013. Thresholds were calculated from the histogram in Figure 2. Pixels within the class 5 range represent fishing vessel lights. Classes 1–4 represent reflected light from ocean water or light from cloud cover.

Month	Class 1	Class 2	Class 3	Class 4	Class 5
August	10	17	23	30	40
September	9	16	22	28	38
October	8	14	19	27	38
November	8	13	19	28	38
December	7	12	18	27	38

Table 3

Mean monthly sea-surface temperature (SST) values (°C) and standard deviations (SD), used to distinguish the light of vessels fishing for Pacific saury (*Cololabis saira*) from the lights of fishing fleets fishing for other fish. All lights occurring below the upper SST limit were categorized as locations of vessels targeting Pacific saury.

Month	Mean	SD	Upper SST limit
August	20.79	2.69	23.48
September	18.89	2.47	21.36
October	15.90	2.58	18.48
November	14.56	2.88	17.44
December	13.60	2.89	16.49

produced and distributed by Archiving Validation and Interpretation of Satellite Oceanographic Data (AVISO; website) at a spatial resolution of 0.33°×0.33°. The surface geostrophic velocities were used to compute for EKE by using the following equation (Steele et al., 2010):

$$EKE = ½ (u'^2 + v'^2), \qquad (2)$$

where u' and v' = the zonal and meridional components of geostrophic currents, respectively.

With the grid function of the software package Generic Mapping Tools, vers. GMT 4.5.7 (website),we were able to calculate the monthly averages for each environmental variable from daily data sets, resampled to 1-km resolution and converted to Esri ASCII grid format(Esri, Redlands, CA) or to comma-separated values (CSV) format, as required by the software program Maxent (website).

Construction of a maximum entropy model

To develop a model with a maximum entropy approach, we used the software program Maxent, vers. 3.3.3k. Phillips et al. (2006) provided detailed information on the mode of operating this software. We constructed models using default values for regulation parameter (1), maximum iteration (500), and automatic feature class selection. We used a cross-validation procedure to evaluate the performance of the models. For background points, we generated pseudo-absences (10:1 ratio of pseudo-absence to presence) following Barbet-Massin et al., (2012) on the basis of random spatial sampling within the study area (excluding points of presence of Pacific saury). We used the *density.tools. RandomSample* command line in Maxent to generate the random pseudo-absences. For each monthly model, the data were randomly split into 2 categories: one category for training data (70%) and one for test data (30%). The test points were then used to calculate the area under the curve (AUC) of the receiver operating characteristic (ROC) (Phillips et al., 2006).

Evaluation and validation of the model

We used the AUC metric of the ROC curve to evaluate model fit (Elith et al., 2006; Phillips et al., 2006). The relative contribution of individual environmental variables within the maximum entropy model was examined by using the heuristic estimates of variable importance based on the increase in the model gain, which is associated with each environmental factor and its corresponding model feature. Response curves generated for each factor were examined to derive the favorable environmental ranges for potential fishing zones.

Independent sets of monthly OLS data from 2011 through 2013 were used to validate the models. The base models were used to create habitat suitability indices (HSIs) that assimilated similar environmental layers for the corresponding period from 2011 through 2013. Spatial HSI maps were generated and overlain with information on OLS data from the period 2011–2013.

Results

Spatiotemporal distribution of fishing locations, and environmental data

Figure 3 shows the variation in the distribution of fishing vessel lights from August through December during 2005–2013. Vessels started to appear off the Kuril Islands and east of Hokkaido in August (Fig. 3A). At the same time, fishing also occurred around the Sanriku coast of Japan and an offshore area between 150°E and 41°N that extended northeast to155°E and 43°N.

During September (Fig. 3B), fishing vessels were distributed mostly north of 42°N, especially off east-
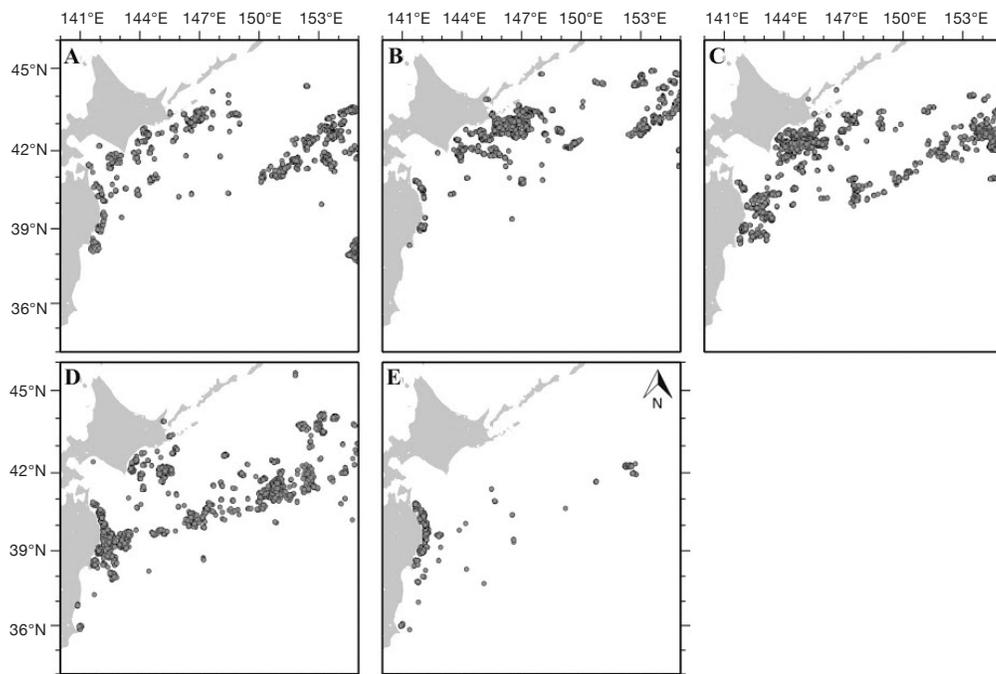
Figure 3

Spatial distribution of fishing locations for Pacific saury (*Cololabis saira*) in the western North Pacific pooled during (**A**) August, (**B**) September, (**C**) October, (**D**) November, and (**E**) December for the period 2005–2013.

ern Hokkaido, whereas the number of vessels off the Sanriku coast decreased. In October (Fig. 3C), fishing vessels were widely distributed in Hokkaido and Sanriku waters. The distribution of fishing vessels moved slightly to the south and approached the shores of southeastern Hokkaido and Sanriku (38–41°N). During this same month, the offshore fishing locations (148°E and 48°N) also increased and extended northeast to 154°E and 43°N.

During November (Fig. 3D), fishing vessels moved southward. The number of fishing vessels in eastern Hokkaido waters decreased, but the number of fishing vessels around the Sanriku coast increased (38–41°N) and moved northeast to 155°E and 43°N. A small number of fishing vessels also appeared off the Joban coast. In December (Fig. 3E), fishing vessels appeared mostly along the Sanriku coast and were distributed in near-shore waters between 38°N and 40°N; however, a small number of fishing vessels still remained offshore and along the Joban coast.

The monthly averaged time series of environmental data for the period 2005–2013 are shown in Figure 4. Mean SST values indicated a decreasing trend of temperature on the fishing locations from August through December (Fig. 4A). Mean chl-*a* concentrations (Fig. 4B) increased in September but declined in December. The mean chl-*a* concentration was highest in September (0.93 mg/m³), when most vessels were concentrated off the eastern coast of Hokkaido and near the southern Kuril Islands. Mean EKE and SSHA values (Fig. 4,

C–D) increased in trends that corresponded with the southward shift of fishing vessels, especially from September until November.

Model performance and potential fish habitat

All monthly maximum entropy models significantly fitted better than they were fitted by chance as supported by the modest values of the performance metric (AUC>0.5; Table 4). This outcome indicates the high predictive success of these models (Elith et al., 2006; Phillips et al., 2006). The relative contribution of each environmental variable to model prediction is shown in Table 5. Model results indicate that the 2 most important factors in August and October were SST and EKE, and in September the most important factors were SST and chl-*a*. In November and December, the 2 highest contributions to model gain were SST and SSHA.

Figure 5 provides the model-derived preferred ranges for each environmental variable. The plots in this figure show the performance and contribution of the various environmental data to model fit. High probabilities of occurrence of Pacific saury were observed in varied ranges for each month. In general, occurrence of Pacific saury had the highest probabilities in cool (14–16ºC) waters with chl-*a* concentrations of 0.5–2.0 mg/m³. In addition, there were high probabilities of occurrence of Pacific saury at low to moderate EKE and positive SSHA values.

Figure 4

Monthly mean time series of (**A**) sea-surface temperature (SST), (**B**) chlorophyll-*a* (chl-*a*), (**C**) sea-surface height anomaly (SSHA), and (**D**) eddy kinetic energy (EKE) in the western North Pacific from August through December for the period 2005–2013.
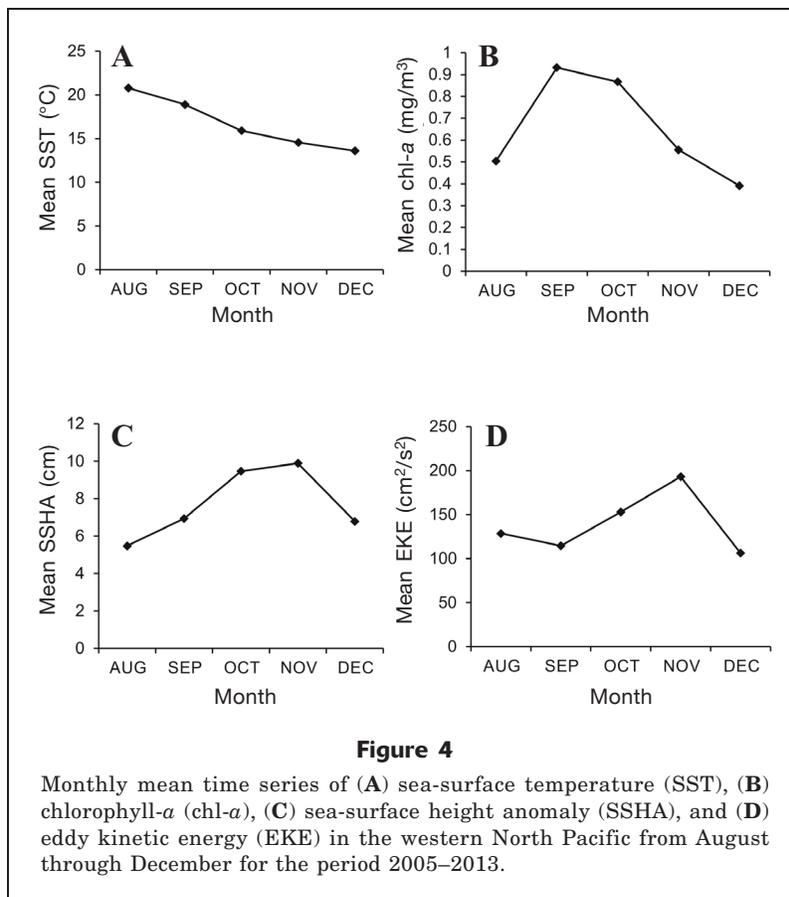
Table 4

Summary statistics derived from the monthly models for the period 2005–2010. The base models were calibrated with 70% of Pacific saury occurrence data, and values for the area under the curve (AUC) were calculated from the remaining 30% of the occurrence data. The total number of fishing locations (*N*) is given for each month. All the models fitted significantly better than if they were fitted by chance (AUC>0.5).

Month	AUC	*N*
August	0.907	8074
September	0.910	7411
October	0.912	10,062
November	0.886	5162
December	0.949	429

Table 5

Heuristic estimates of the relative percent contribution of environmental variables to models derived by using a maximum entropy approach. The 2 most important variables for each monthly model are presented in bold. SST=sea surface temperature; chl-*a*=chlorophyll-*a*; EKE=eddy kinetic energy; SSHA=sea-surface height anomaly.

	Environmental predictors			
Model	SST	Chl-*a*	EKE	SSHA
August	**55.6**	7.1	**28.1**	9.2
September	**56.8**	21.6	14.4	7.2
October	**72.2**	5.9	**13.6**	8.3
November	**73.2**	2.9	9.4	**14.5**
December	**57.6**	0.8	6.2	**35.4**

Prediction and validation of occurrence

Maps of predicted HSI for August–December (2011–2013) are shown in Figure 6. In August, the predicted probability of occurrence of Pacific saury covered the entire Oyashio region, but it did so with a small value of HSI (Fig. 6, A–C). In September, high probability areas (HIS ≥0.6) increased, especially east of Hokkaido and the Kuril Islands. The presence of fishing locations derived from OLS images also increased east of Hokkaido during this period (Fig. 6, D–F). In October, the known peak of the fishing season, a high

Figure 5

Response curves from the monthly base model for (**A**) chlorophyll-*a* (chl-*a*), (**B**) sea surface temperature (SST), (**C**) eddy kinetic energy (EKE), and (**D**) sea-surface height anomaly (SSHA) in the western North Pacific. The error margin (EM) for each plot is provided.
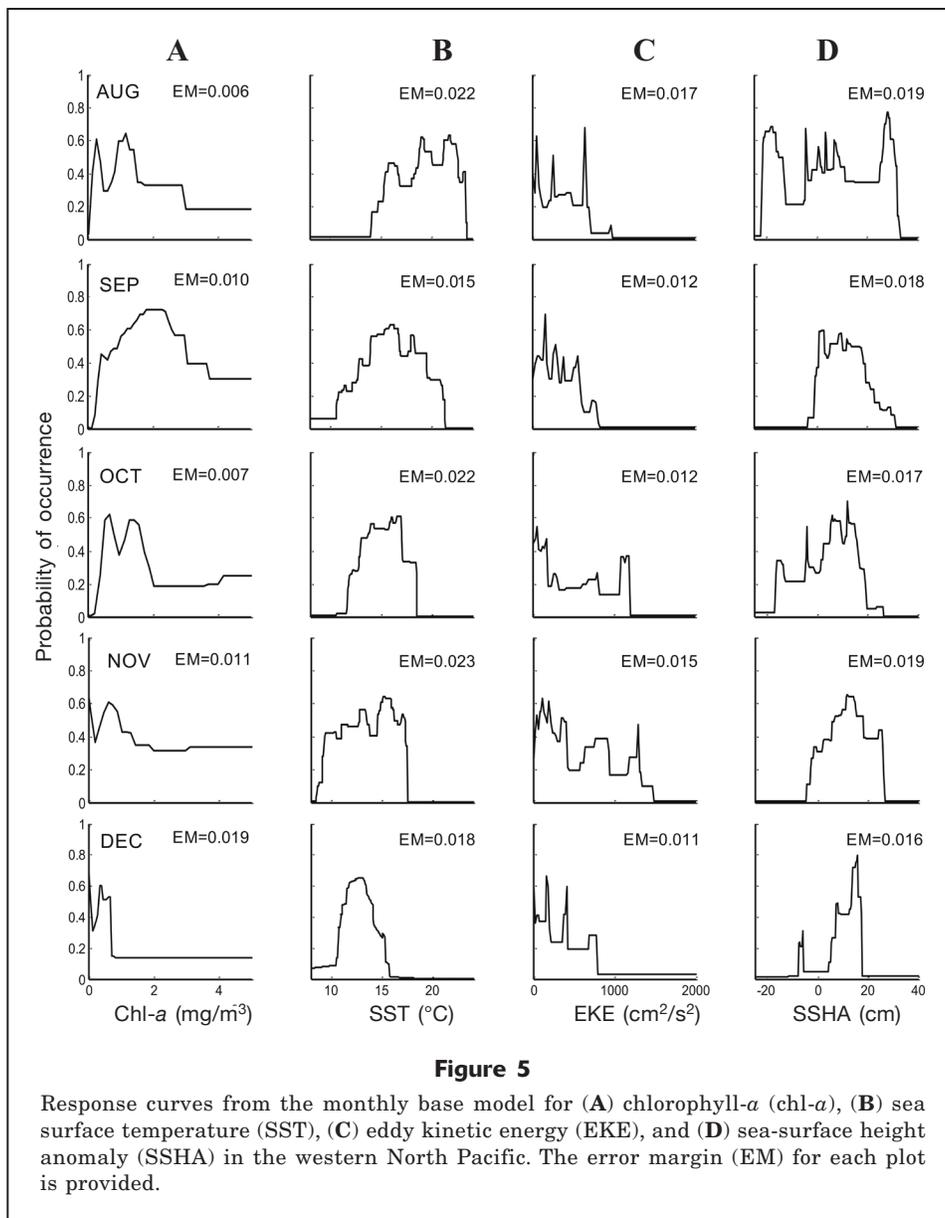
probability of occurrence of Pacific saury remained for east and southeast of Hokkaido and south of the Kuril Islands. During the same month, the results from the predicted HSI indicated the Kuroshio–Oyashio transition zone at 40°N, and a correspondingly high probability of occurrence of Pacific saury (Fig. 6, G–I). In November, the high predicted HSI in the transition zone (38–42°N and 142–155°E) increased, especially off the Sanriku (39–41°N) and Joban (38–39°N) coasts (Fig. 6, J–L). At the end of the fishing season in December, the predicted probability of occurrence dramatically decreased in the offshore areas but remained high off the Sanriku and Joban coasts (Fig. 6, M–O). In general, the distribution of Pacific saury based on the HSI showed moderate spatial correlation with actual fishing locations derived from OLS imag-

es, although it did so with relatively low HSI values, particularly in August.

Discussion

We used fishing locations for Pacific saury and oceanographic variables with maximum entropy models to predict the potential fishing zones for Pacific saury in western North Pacific waters. Analyses of OLS nighttime images allowed us to locate fishing vessel lights across space and time, and we assumed that Pacific saury were caught in areas where fishing vessels were identified. On the basis of the derived fishing vessel locations, we were able to estimate the spatial and temporal distribution of potential fishing zones for Pacific saury.
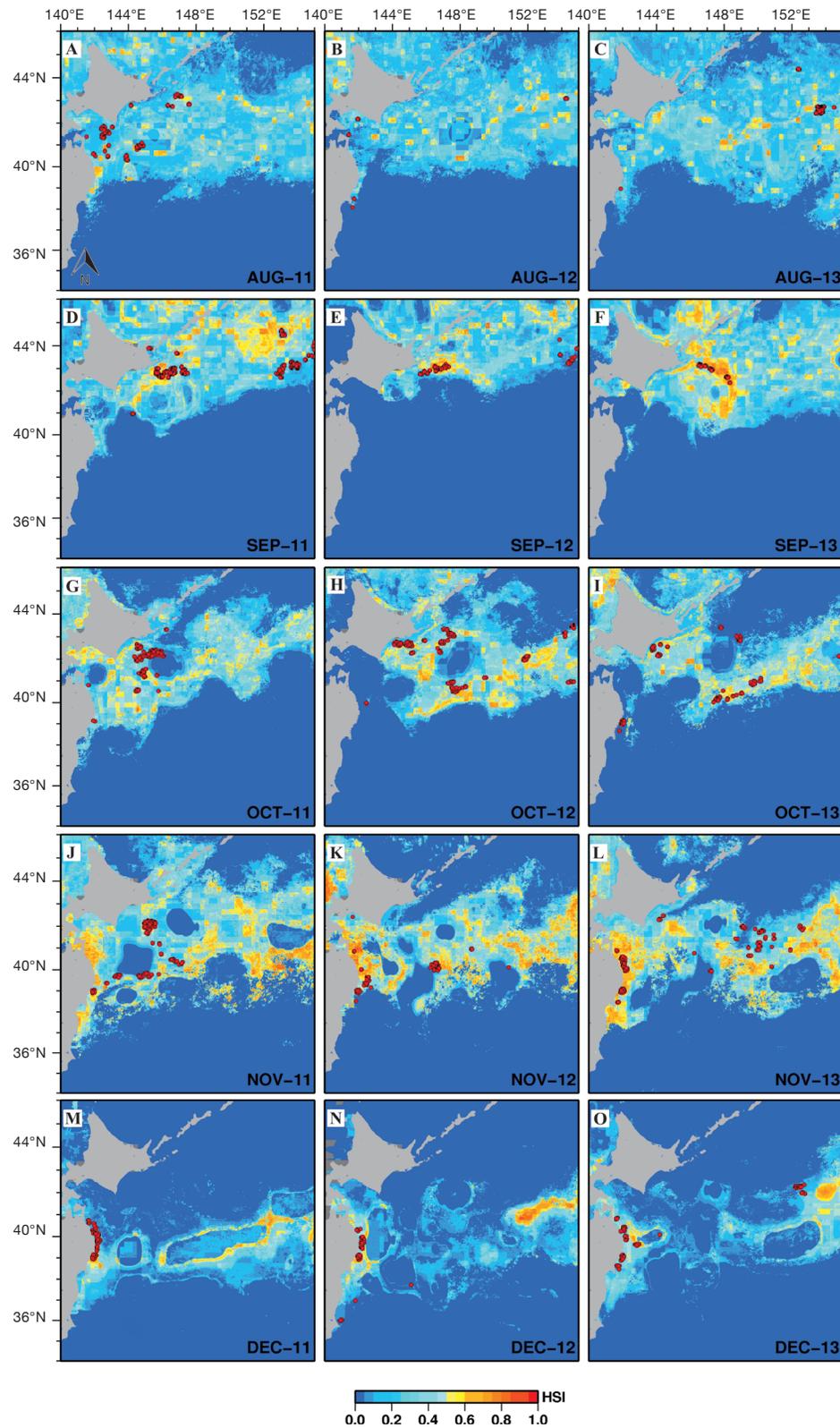
Figure 6

The spatial distribution of fishing locations (red dots) for Pacific saury (*Cololabis saira*) in the western North Pacific derived from analyses of images from the Operational Linescan System of the U.S. Defense Meteorological Satellite Program for the period August–December during 2011–2013, overlain on maps of habitat suitability predicted with base models. The suitability is depicted as an Habitat Suitability Index (HSI) score ranging from 0 to 1, representing "poor" to "good" habitat quality, respectively.

At the beginning of the fishing season, fishing locations derived from OLS images showed that most of the vessels that fished for Pacific saury appeared east of Hokkaido and south of the Kuril Islands (Fig. 3, A and B). In the middle of the fishing season (October to November) (Fig. 3, C and D), vessels that fish for Pacific saury moved slightly to the south and appeared mostly around the eastern coasts of Hokkaido and Sanriku—a finding that potentially resulted from the southward extension of Oyashio fronts (Watanabe et al., 2006; Tseng et al., 2011). At the end of the fishing season, vessels that fish for Pacific saury were concentrated along the Sanriku coast (Fig. 3E).

Images from the OLS also showed that some of the fishing vessels appeared outside the EEZ, possibly because Pacific saury is an oceanic spawner, unlike other small pelagic fishes, such as the Japanese sardine (*Sardinops melanostictus*) and the Japanese anchovy (*Engraulis japonicus*), that generally spawn in the coastal and near shore waters of Japan (Zenitani et al., 1995). The low capture of fish west of 150°E from June through July before the fishing season indicates that Pacific saury caught by Japanese fishing vessels were located far from the northeastern coasts of Japan (Tohoku National Fisheries Research Institute[3]).

The predicted distribution of Pacific saury in the western North Pacific revealed areas of high probability of occurrence off Hokkaido and the Kuril Islands (Fig. 6, A–F), areas that gradually moved south toward the Sanriku and Joban coasts by the end of the fishing season (Fig. 6, M–O). These patterns coincided with the north–south migration of Pacific saury that marks the start and end of the fishing season. Results from a maximum entropy approach further indicate that the highest probability of presence occurred along the Kuroshio–Oyashio transition zone in November (Fig. 6, J–L).

The occurrence of large-size Pacific saury (>29.0 cm in knob length) off the southern Kuril Islands during their spawning migration indicates that a high proportion of large-size Pacific saury moved from the high seas to coastal waters at the beginning of their migration toward the southwest—movement that was then followed by a similar migration of medium-size Pacific saury (24.0–29.0 cm in knob length). Therefore, abundance of Pacific saury off the coastal waters in our study is higher than the abundance observed in regions in the high seas (Huang, 2010). In addition, the high density of Pacific saury off Hokkaido and the Kuril Islands was probably related to the southward movement of the Oyashio Current (Tseng et al., 2011). The high presence of Pacific saury at the coasts also could be a result of a westward current intensification, which can result in the formation of oceanic fronts (Huang, 2010). These frontal features have been known as the

preferred migratory routes of Pacific saury and other marine species (Saitoh et al., 1986; Zainuddin et al., 2008).

Although oceanographic conditions are likely to affect species distribution, other factors, such as prey density, are equally important. In the Kuroshio–Oyashio transition zone, Oyashio intrusions transport organic matter, thereby supporting the production of copepods, which are the primary prey of Pacific saury (Odate, 1994; Shimizu et al., 2009). This salient physical process could potentially explain the existence of habitat areas of Pacific saury in the transition zone, areas that were identified with maximum entropy models and that consequently highlight the importance of this region as migratory and feeding corridors for Pacific saury.

The variability of the performance of the maximum entropy model was very low across the monthly base models, where AUCs higher than 0.9 indicate that models had excellent agreement with the test data (Table 4). As pointed out earlier, productivity and fish distribution are influenced by changes in the environment evident from the variations in temperature, currents, salinity, and wind fields (Southward et al., 1988; Alheit and Hagen, 1997). In our study, SST (among the set of oceanographic variables examined) showed the highest contribution to all monthly base models (Table 5), indicating the sensitivity of Pacific saury to temperature changes. For instance, increasing SST will directly reduce juvenile growth and prevent, or delay, the southern migration of Pacific saury in winter (Ito et al., 2013). Moreover, changes in winter SSTs in the Kuroshio–Oyashio transition zone and in the Kuroshio and Oyashio regions also affected the abundance of the large-size (winter cohort) and medium-size (spring cohort) groups of Pacific saury (Tian et al., 2003).

To our knowledge, this study was the first attempt to use both EKE and SSHA to describe potential fishing habitat of Pacific saury in relation to mesoscale oceanography variability. Our results indicate that fishing activities occurred in areas with low to moderate EKE (Fig. 5), reflecting the likely association of this species with eddies. Meandering eddies likely trap prey of Pacific saury, creating good feeding opportunities through local enhancement of chl-*a* and zooplankton abundance and through the aggregation of prey organisms (Owen, 1981; Zhang et al., 2001). The importance of forage availability for Pacific saury is further reflected in the higher contribution of chl-*a* concentration to the base model in September (Table 5). Together with SST, chl-*a* has been found to influence Pacific saury growth, recruitment, distribution, and migratory patterns (Ito et al., 2004; Oozeki et al., 2004; Yasuda and Watanabe, 2007). However, from November through December, the distribution of Pacific saury likely is not limited by food availability because of a general increase in ocean mixing and a decrease in water column stratification during this period. These oceanographic conditions consequently enhance the chl-*a* concentration in the mixed-water region (Mugo et al., 2014).

---

[3] Tohoku National Fisheries Research Institute. 2010. The 58th Annual Report of the Research Meeting on Saury Resources, 250 p. Tohoku Natl. Fisheries Res. Inst., Hachinohe, Japan. [In Japanese.]

Finally, OLS nighttime images were found to be useful for investigating the distribution of the lights of fishing vessels—an outcome that supports the results of earlier studies (Semedi et al., 2002; Saitoh et al., 2010). However, cloud contamination significantly limited the use of OLS images and reduced the density of proxy fishing locations; therefore, logbook data are needed to confirm the validity of fish occurrences in the future. The integration of these empirical data with multi sensor remote sensing information within a modeling platform could offer a powerful and innovative way to identify the potential fishing zones for Pacific saury and could be used to support fisheries management decisions.

Acknowledgments

Literature cited

Alabia, I. D., S. Saitoh, R. Mugo, H. Igarashi, Y. Ishikawa, N. Usui, M. Kamachi, T. Awaji, and M. Seito.
　2015.　Seasonal potential fishing ground prediction of neon flying squid (*Ommastrephes bartramii*) in the western and central North Pacific. Fish. Oceanogr. 24:190–203.　Article

Alheit, J., and E. Hagen.
　1997.　Long-term climate forcing of European herring and sardine populations. Fish. Oceanogr. 6:130–139.　Article

Ayers, J. M., and M. S. Lozier.
　2010.　Physical controls on the seasonal migration of the North Pacific transition zone chlorophyll front. J. Geophys. Res. 115:C05001.　Article

Barbet–Massin, M., F. Jiguet, C. H. Albert, and W. Thuiller.
　2012.　Selecting pseudo-absences for species distribution models: how, where and how many? Methods Ecol. Evol. 3:327–338.　Article

Belkin, I. M., and Y. G. Mikhailichenko.
　1986.　Thermohaline structure of the Northwest Pacific Frontal Zone near 160° E. Oceanology [English translation.] 26:47–49.

Belkin, I. M., V. A. Bubnov, and S. E. Navrotskaya.
　1992.　Ocean fronts of "Megapolygon-87." *In* The Megapolygon experiment (Y. A. Ivanov, ed.), p. 96–111. Nauka, Moscow. [In Russian.]

Belkin, I., R. Krishfield, and S. Honjo.
　2002.　Decadal variability of the North Pacific Polar Front: subsurface warming versus surface cooling. Geophys. Res. Lett. 29:65-1–65-4.　Article

Edrén, S. M. C., M. S. Wisz, J. Teilmann, R. Dietz, and J. Söderkvist.
　2010.　Modelling spatial patterns in harbour porpoise satellite telemetry data using maximum entropy. Ecography 33:698–708.　Article

Elith, J., C. H. Graham, R. P. Anderson, M. Dudik, S. Ferrier, A. Guisan, R. J. Hijmans, F. Huettmann, J. R. Leathwick, A. Lehmann, et al.
　2006.　Novel methods improve prediction of species' distributions from occurrence data. Ecography 29:129–151.　Article

Elvidge, C. D., K. E. Baugh, E. A. Kihn, H.W. Kroehl, and E.R. Davis.
　1997.　Mapping city lights with nighttime data from the DMSP Operational Linescan System. Photogramm. Eng. Remote Sens. 63:727–734.

Fisheries Agency and Fisheries Research Agency of Japan.
　2012.　Marine fisheries stock assessment and evaluation for Japanese waters (fiscal years 2011/2012), 1743 p. Fisheries Agency and Fisheries Research Agency of Japan, Tokyo. [In Japanese.]

Fukushima, S.
　1979.　Synoptic analysis of migration and fishingconditions of saury in northwest Pacific Ocean. Bull. Tohoku Reg. Fish Res. Lab. 41:1–70. [In Japanese.]

Huang, W.-B.
　2010.　Comparisons of monthly and geographical variations in abundance and size composition of Pacific saury between the high-seas and coastal fishing grounds in the northwestern Pacific. Fish. Sci. 76:21–31.　Article

Huang, W.-B., N. C. H. Lo, T.-S. Chiu, and C.-S. Chen.
　2007.　Geographical distribution and abundance of Pacific saury, *Cololabis saira* (Brevoort) (Scomberesocidae), fishing stocks in the northwestern Pacific in relation to sea temperature. Zool. Stud. 46:705–716.

Ito, S., H. Sugisaki, A. Tsuda, O. Yamamura, and K. Okuda.
　2004.　Contributions of the VENFISH program: mesozooplankton, Pacific saury (*Cololabis saira*) and walleye pollock (*Theragra chalcogramma*) in the northwestern Pacific. Fish. Oceanogr. 13 (suppl. S1):1–9.　Article

Ito, S.-I., B. A. Megrey, M. J. Kishi, D. Mukai, Y. Kurita, Y. Ueno, and Y. Yamanaka.
　2007.　On the interannual variability of the growth of Pacific saury (*Cololabis saira*): a simple 3-box model using NEMURO.FISH. Ecol. Model. 202:174–183.　Article

Ito, S.-I., T. Okunishi, M. J. Kishi, and M. Wang.
　2013.　Modelling ecological responses of Pacific saury (*Cololabis saira*) to future climate change and its uncertainty. ICES J. Mar. Sci. 70:980–990.　Article

Johnson, C. J., and M. P. Gillingham.
　2005.　An evaluation of mapped species distribution models used for conservation planning. Environ. Conserv. 32:117–128.　Article

Kitano, K.
　1972.　On the polar frontal zone of the northern North Pacific Ocean. *In* Biological oceanography of the northern North Pacific Ocean (A.Y. Takenouti, ed.), p. 73–82. Idemitsu Shoten, Tokyo.

Kiyofuji, H., and S. Saitoh.
　2004.　Use of nighttime visible images to detect Japanese common squid *Todarodes pacificus* fishing areas and potential migration routes in the Sea of Japan. Mar. Ecol. Prog. Ser. 276:173–186.　Article

Kiyofuji. H., K. Kumagai, S. Saitoh, Y. Arai, and K. Sakai.
　2004.　Spatial relationship between Japanese common squid (*Todarodes pacificus*) fishing grounds and fishing ports: an analysis using remote sensing and geographical information systems. *In* GIS/spatial analyses in fishery

and aquatic sciences, vol. 2 (T. Nishida, P. J. Kaiola, and C. E. Hollingworth, eds.), p 341–354. Fishery-Aquatic GIS Research Group, Saitama, Japan.

Kosaka, S.
    2000. Life history of Pacific saury, *Cololabis saira,* in the Northwest Pacific and consideration of resource fluctuation based on it. Bull. Tohoku Natl. Fish. Res. Inst. 63:1–96. [In Japanese with English abstract.]

Miyake, H.
    1989. Water mass structure and the salinity minimum waters in the western subarctic boundary region of North Pacific. Umi to Sora 65:107–118. [In Japanese.]

Mugo, R. M., S. Saitoh, F. Takahashi, A. Nihira, and T. Kuroyama.
    2014. Evaluating the role of fronts in habitat overlaps between cold and warm water species in the western North Pacific: a proof of concept. Deep-Sea Res., II 107:29–39. Article

Mukai, D., M. J. Kishi, S. Ito, and Y. Kurita.
    2007. The importance of spawning season on the growth of Pacific saury: a model-based study using NEMURO. FISH. Ecol. Model. 202:165–173. Article

Murase, H., T. Hakamada, K. Matsuoka, S. Nishiwaki, D. Inagake, M. Okazaki, N. Tojo, and T. Kitakado.
    2014. Distribution of sei whales (*Balaenoptera borealis*) in the subarctic–subtropical transition area of the western North Pacific in relation to oceanic fronts. Deep-Sea Res., II 107:22–28. Article

Odate, K.
    1994. Zooplankton biomass and its long-term variation in the western North Pacific Ocean, Tohoku sea area, Japan. Bull. Tohoku Natl. Fish Res. Inst. 56:115–163. [In Japanese with English abstract.]

Onishi, H.
    2001. Spatial and temporal variability in a vertical section across the Alaskan Stream and Subarctic Current. J. Oceanogr. 57:79–91. Article

Oozeki, Y., Y. Watanabe, and D. Kitagawa.
    2004. Environmental factors affecting larval growth of Pacific saury, *Cololabis saira*, in the northwestern Pacific Ocean. Fish. Oceanogr. 13(suppl. S1):44–53. Article

Owen, R.W.
    1981. Fronts and eddies in the sea: mechanisms, interactions and biological effects. *In* Analysis of marine ecosystems (A. R. Longhurst, ed.),p. 197–233. Academic Press, New York.

Peterson, A.T., M. Papes, and M. Eaton.
    2007. Transferability and model evaluation in ecological niche modeling: a comparison of GARP and Maxent. Ecography 30:550–560. Article

Polovina, J. J., and E. A. Howell.
    2005. Ecosystem indicators derived from satellite remotely sensed oceanographic data for the North Pacific. ICES J. Mar. Sci. 62:319–327. Article

Phillips, S. J., R. P. Anderson, and R. E. Schapire.
    2006. Maximum entropy modeling of species geographic distributions. Ecol. Model. 190:231–259. Article

Ready, J., K. Kaschner, A. B. South, P. D. Eastwood, T. Rees, J. Rius, E. Agbayani, S. Kullander, and R. Froese.
    2010. Predicting the distributions of marine organisms at the global scale. Ecol. Model. 221:467–478. Article

Roden, G. I.
    1991. Subarctic-subtropical transitional zone of the North Pacific: large-scale aspects and mesoscale structure. *In* Biology, oceanography, and fisheries of the North Pacific transitional zone and subarctic frontal zone. NOAA Tech. Rep. NMFS 105 (J. A. Wetherall, ed.), p. 1–38.

Roden, G. I., B. A. Taft, and C. C. Ebbesmeyer.
    1982. Oceanographic aspects of the Emperor Seamounts region. J. Geophys. Res., C 87:9537–9552. Article

Saitoh, S.,-I. A. Fukaya, K. Saitoh, B. Semedi, R. Mugo, S. Matsumura, and F. Takahashi.
    2010. Estimation of number of Pacific saury fishing vessels using night-time visible images. Int. Arch. Photogramm. Remote Sens. Spatial Inf. Sci. 38:1013–1016.

Saitoh, S., S. Kosaka, and J. Iisaka.
    1986. Satellite infrared observations of Kuroshio warmcore rings and their application to study of Pacific saury migration. Deep-Sea Res., A33:1601–1615. Article

Sakurai, Y.
    2007. An overview of the Oyashio ecosystem. Deep-Sea Res., II 54:2526–2542. Article

Semedi, B., S.-I. Saitoh, K. Saitoh, and K. Yoneta.
    2002. Application of multi-sensor satellite remote sensing for determining distribution and movement of Pacific saury, *Cololabis saira*. Fish. Sci. 68:1781–1784.

Shimizu, Y., K. Takahashi, S.-I. Ito, S. Kakehi, H. Tatebe, I. Yasuda, A. Kusaka, and T. Nakayama.
    2009. Transport of subarctic large copepods from the Oyashio area to the mixed water region by the coastal Oyashio intrusion. Fish. Oceanogr. 18:312– 327. Article

Shotwell, S. K., D. H. Hanselman, and I. M. Belkin.
    2014. Toward biophysical synergy: investigating advection along the Polar Front to identify factors influencing Alaska sablefish recruitment. Deep-Sea Res., II 107:40–53. Article

Southward, A. J., G. T. Boalch, and L. Maddock.
    1988. Fluctuations in the herring and pilchard fisheries of Devon and Cornwall linked to change in climate since the 16th century. J. Mar. Biol. Assoc. U.K. 68:423–445. Article

Steele, J. H., S. A. Thorpe, and K. K. Turekian (eds.).
    2010. Elements of physical oceanography: a derivative of the Encyclopedia of Ocean Science, 660 p. Academic Press, London.

Takagi, M., and H. Shimoda.
    1991. Handbook of image analysis, 2032 p. Univ. Tokyo Press, Tokyo. [In Japanese.]

Tian, Y., T. Akamine, and M. Suda.
    2002. Long-term variability in the abundance of Pacific saury in the northwestern Pacific Ocean and climate changes during the last century. Bull. Jpn. Soc. Fish. Oceanogr. 66:16–25. [In Japanese with English abstract.]
    2003. Variations in the abundance of Pacific saury (*Cololabis saira*) from the northwestern Pacific in relation to oceanic-climate changes. Fish. Res. 60:439–454. Article
    2004. Modeling the influence of oceanic-climatic changes on the dynamics of Pacific saury in the northwestern Pacific using a life-cycle model. Fish. Oceanogr. 13:125–137. Article

Tohoku National Fisheries Research Institute.
    2010. The 58[th]Annual Report of the ResearchMeeting on Saury Resources. Tohoku National Fisheries Research Institute, Hachinohe, Japan. [In Japanese.]

Tseng, C.-T., C.-L. Sun, S.-Z. Yeh, S.-C. Chen, W.-C. Su, and D. C. Liu.
    2011. Influence of climate-driven sea surface temperature increase on potential habitats of the Pacific saury (Cololabis saira). ICES J. Mar. Sci. 68:1105–1113. Article

Tseng, C.-T., N.-J. Su, C.-L. Sun, A. E. Punt, S.-Z. Yeh, D.-C. Liu, and W.-C. Su.
  2013   Spatial and temporal variability of the Pacific saury (*Cololabis saira*) distribution in the northwestern Pacific Ocean. ICES J. Mar. Sci. 70:991–999. Article

Tsoar, A., O. Allouche, O. Steinitz, D. Rotem, and R. Kadmon.
  2007. A comparative evaluation of presence only methods for modelling species distribution. Diversity Distrib. 13:397–405. Article

Waluda, C. M., P. N. Trathan, C. D. Elvidge, V. R. Hobson, and P. G. Rodhouse.
  2002. Throwing light on straddling stocks of *Illex argentinus*: assessing fishing intensity with satellite imagery. Can. J. Fish. Aquat. Sci. 59:592–596. Article

Watanabe, K., E. Tanaka, S. Yamada, and T. Kitakado.
  2006. Spatial and temporal migration modeling for stock of Pacific saury, *Cololabis saira* (Brevoort), incorporating effect of sea surface temperature. Fish. Sci. 72:1153–1165. Article

Yasuda, I., and Y. Watanabe.
  1994. On the relationship between the Oyashio front and saury fishing grounds in the north-western Pacific: a forecasting method for fishing ground locations. Fish. Oceanogr. 3:172–181. Article
  2007. Chlorophyll *a* variation in the Kuroshio Extension revealed with a mixed-layer tracking float: implication on the long-term change of Pacific saury (*Cololabis saira*). Fish. Oceanogr. 16:482–488. Article

Yatsu, A., S. Chiba, Y. Yamanaka, S.-I. Ito, Y. Shimizu, M. Kaeriyama, and Y. Watanabe.
  2013. Climate forcing and the Kuroshio/Oyashio ecosystem. ICES J. Mar. Sci. 70:922–933. Article

Yoshida, T.
  1993. Oceanographic structure of the upper layer in the western North Pacific subarctic region and its variation. PICES Sci. Rep. 1:38–41.

Zainuddin, M., K. Saitoh, and S.-I. Saitoh.
  2008. Albacore (*Thunnus alalunga*) fishing ground in relation to oceanographic conditions in the western North Pacific Ocean using remotely sensed satellite data. Fish. Oceanogr. 17:61–73. Article

Zenitani, H., M. Ishida, Y. Konishi, T. Goto, Y. Watanabe, and R. Kimura.
  1995. Distributions of eggs and larvae of Japanese sardine, Japanese anchovy, mackerels, round herring, Japanese horse mackerel, and Japanese common squid in the waters around Japan, 1991 through 1993. Natl. Res. Inst., Fish. Agency Jap., Res. Manage. Res. Rep. Ser. A-1, 368 p.

Zhang, J.-Z., R. Wanninkhof, and K. Lee.
  2001. Enhanced new production observed from the diurnal cycle of nitrate in an oligotrophic anticyclonic eddy. Geophys. Res. Lett. 28:1579–1582. Article